JOURNAL OF VIROLOGY, Jan. 2005, p. 503–511 Vol. 79, No. 1
0022-538X/05/$08.00+0 doi:10.1128/JVI.79.1.503–511.2005

Severe Acute Respiratory Syndrome Coronavirus Infection of Golden Syrian Hamsters

Anjeanette Roberts,[1]* Leatrice Vogel,[1] Jeannette Guarner,[2] Norman Hayes,[2] Brian Murphy,[1] Sherif Zaki,[2] and Kanta Subbarao[1]

Laboratory of Infectious Diseases, National Institute of Allergy and Infectious Disease, National Institutes of Health, Bethesda, Maryland,[1] and Infectious Disease Pathology Activity, National Center for Infectious Diseases, Centers for Disease Control and Prevention, Atlanta, Georgia[2]

Received 3 June 2004/Accepted 27 August 2004

Small animal models are needed in order to evaluate the efficacy of candidate vaccines and antivirals directed against the severe acute respiratory syndrome coronavirus (SARS CoV). We investigated the ability of SARS CoV to infect 5-week-old Golden Syrian hamsters. When administered intranasally, SARS CoV replicates to high titers in the lungs and nasal turbinates. Peak replication in the lower respiratory tract was noted on day 2 postinfection (p.i.) and was cleared by day 7 p.i. Low levels of virus were present in the nasal turbinates of a few hamsters at 14 days p.i. Viral replication in epithelial cells of the respiratory tract was accompanied by cellular necrosis early in infection, followed by an inflammatory response coincident with viral clearance, focal consolidation in pulmonary tissue, and eventual pulmonary tissue repair. Despite high levels of virus replication and associated pathology in the respiratory tract, the hamsters showed no evidence of disease. Neutralizing antibodies were detected in sera at day 7 p.i., and mean titers at day 28 p.i. exceeded 1:400. Hamsters challenged with SARS CoV at day 28 p.i. were completely protected from virus replication and accompanying pathology in the respiratory tract. Comparing these data to the mouse model, SARS CoV replicates to a higher titer and for a longer duration in the respiratory tract of hamsters and is accompanied by significant pathology that is absent in mice. Viremia and extrapulmonary spread of SARS CoV to liver and spleen, which are seen in hamsters, were not detected in mice. The hamster, therefore, is superior to the mouse as a model for the evaluation of antiviral agents and candidate vaccines against SARS CoV replication.

Severe acute respiratory syndrome coronavirus (SARS CoV) is an animal coronavirus that caused an outbreak of SARS in humans in 2002 to 2003 (5, 13, 14, 18, 26) following introduction from a yet-unidentified natural reservoir. SARS CoV has been isolated from masked palm civets (*Paguma larvata*) and raccoon dogs (*Nyctereutes procyonoides*) (10), weasel-like animals that are indigenous to Guangdong Province in southeast China, where SARS CoV-associated infection of humans was first reported in early 2003 (10, 13). These animals were procured from an exotic animal market in Shenzhen, Guangdong Province, and evidence of infection was established by virus isolation and by detection of SARS CoV genetic material in nasal and/or fecal swabs (10). Antibodies specific for SARS CoV were also identified in sera of masked palm civets, raccoon dogs, and Chinese ferret-badgers (*Melogale moschata*) (10). Viral nucleic acid has also been detected by reverse transcription-PCR in rat droppings and throat and/or rectal swabs from five household cats, a dog, and a rat in a Hong Kong apartment complex where several residents developed SARS (17). In contrast to the host range specificity reported for many coronaviruses, SARS CoV appears to have a broad host range in that it replicates in humans, palm civets, and raccoon dogs and has also been shown to replicate in experimentally infected mice, ferrets, cats, and nonhuman primates (14, 16, 23). The host and tissue ranges of viruses are determined in part by the distribution of viral receptors. The role of a recently identified receptor for SARS CoV, angiotensin-converting enzyme 2 (15), as a determinant of the host range of SARS CoV remains to be determined. The presence of angiotensin-converting enzyme 2 homologs in a wide range of species (4, 12) may account for the broad host range of SARS CoV.

Since SARS CoV was identified as the causative agent for SARS (8), investigators have been working diligently to develop vaccines and antiviral therapies to prevent and protect against SARS infections. The ~10% mortality associated with the SARS outbreak in 2002 to 2003, the rapidity of international spread (encompassing over 20 countries within weeks of the first reported case), reports of super-spreaders (infected individuals who served as the source for eight or more subsequent infections), and the apparent ease of transmission between individuals from community-acquired infections and one instance of a laboratory-acquired infection highlight the seriousness of this pathogen. In addition to implementing isolation of patients with confirmed SARS cases and quarantine of those with suspected cases, public health officials in China have taken severe steps to prevent the reemergence of SARS in 2003 to 2004 through the culling of thousands of civet cats (a presumed viral reservoir) in Guangdong Province, rapid contact tracing of confirmed SARS patients, and the use of personal protective equipment by health care workers caring for SARS patients. To date only four community-acquired cases of SARS have been reported in 2003 to 2004, suggesting that these interventions may be successful. Although factors such as the genetic sequence of the virus could also explain the mild

* Corresponding author. Mailing address: Laboratory of Infectious Diseases, NIAID, Bldg. 50, Room 6513, 50 South Dr., MSC 8007, Bethesda, MD 20892. Phone: (301) 496-3490. Fax: (301) 496-8312. E-mail: ajroberts@niaid.nih.gov.

illnesses and lack of spread noted in cases in 2004, concerns remain that SARS CoV may reemerge by jumping from an animal host to humans. Therefore, the generation of vaccines and antiviral therapies remains a high priority.

Much effort has been made to identify appropriate animal models for the characterization of SARS CoV replication and associated disease. Such models hold interest for several reasons. First, an exploration of the range of species susceptible to SARS CoV infection may help identify the natural reservoir and potential chains of transmission that occur in nature and may help to focus public health interventions, limiting transmission to human populations in specific geographic areas. Second, the identification of various animal models will facilitate the evaluation of a wider range of virus-vectored vaccines. These live, attenuated virus vectors expressing SARS proteins may be restricted in replication in murine models or restricted by the high cost and specialized facilities needed for evaluation in nonhuman primates. Third, the consequences of SARS CoV infection in a variety of animal models may vary significantly, to include viral replication in the absence of clinical and histopathological illness, viral replication with pathological evidence of disease but absence of clinical illness, or viral replication with both pathological and clinical evidence of illness. The use of different animal models will therefore offer a broader range of parameters for pathogenesis studies, evaluation of antiviral treatments, and vaccine efficacy studies than would a single animal model, and the choice of animal model employed can be tailored to suit the needs of the investigation. Furthermore, if efficacy studies cannot be carried out in humans, two animal models may be required for licensure of a vaccine (7).

One specific example of viruses that are being developed as potential live, attenuated vaccine vectors are the parainfluenza virus types 1, 2, and 3 and a bovine-human parainfluenza virus chimera (2, 6, 19, 21). Because these vectors have been shown to replicate efficiently and elicit protective immunity in a hamster model (24), we chose to examine hamsters as a potential model for SARS CoV disease and replication and subsequent prophylaxis and immunotherapy.

MATERIALS AND METHODS

Animals, virus, and inoculation. All work with infectious virus and with infected animals was performed in biosafety level 3 facilities by personnel wearing powered air-purifying respirators (HEPA AirMate; 3 M, St. Paul, Minn.). Two studies were performed to evaluate SARS CoV replication in the respiratory tracts of 5-week-old Golden Syrian hamsters from Charles River Laboratories (Wilmington, Mass.). The hamsters were housed three per cage in a biosafety level 3 animal facility. After resting for several days, each hamster was anesthetized with a 0.5-ml intramuscular injection of a cocktail containing 18 ml of Ketaject, 0.6 ml of xylazine, 1.1 ml of glycopyrate, and 0.5 ml of Acepromazine. In a pilot study, 10^3 or 10^5 50% tissue culture infective doses ($TCID_{50}$) of SARS CoV was administered intranasally in a volume of 100 μl to 18 hamsters at each dose. Three hamsters from each group were sacrificed on days 1, 3, 5, 7, and 9 postinfection (p.i.), and virus titers in homogenates of lungs and nasal turbinates (NTs) were determined. The three remaining hamsters from each group were bled at 0, 21, and 28 days p.i. for analysis of SARS-specific serum neutralizing antibodies.

In the follow-up study of 48 female Golden Syrian hamsters, 42 anesthetized hamsters received 100 μl (10^3 $TCID_{50}$) of SARS CoV (Urbani strain) intranasally, and as a control, six hamsters received 100 μl of Leibovitz 15 (L15) medium (Invitrogen, Carlsbad, Calif.) intranasally. Hamsters were euthanatized by lethal intraperitoneal injection with sodium pentobarbital (200 μl/hamster) on designated days. Thirty-six of the 42 SARS CoV-inoculated hamsters were sacrificed (six per day) on days 2, 3, 5, 7, 10, and 14. Lungs, NTs, liver, spleen, kidneys, and intestines were harvested from each hamster at each time point. Tissues from three hamsters per day were snap frozen and stored at −70°C until the end of the study. Organs from the other three hamsters were placed in 10% buffered formalin and processed for histopathology and immunohistochemistry (IHC). One of the six remaining SARS-inoculated hamsters was found dead by apparent cannibalization at day 24 of the experiment. The remaining five SARS-inoculated and six mock-infected hamsters were challenged with 10^3 $TCID_{50}$ of SARS CoV on day 28 of the study and sacrificed 3 days later. Lungs, NTs, livers, spleens, and kidneys were collected and processed for viral titration and pathology studies.

Determination of viral titers and total virus. Tissue samples were homogenized to a final 10% (wt/vol) suspension in L15 medium with piperacillin (Sigma Aldrich Co., St. Louis, Mo.), gentamicin (Invitrogen, Grand Island, N.Y.), and amphotericin B (Quality Biological, Gaithersburg, Md.), which were added to the tissue culture medium at final concentrations of 0.4, 0.1, and 5 mg/liter, respectively. Tissue homogenates were clarified by low-speed centrifugation, and virus titers were determined in Vero cell monolayers in 24- and 96-well plates as described previously (23). Virus titers are expressed as $TCID_{50}$ per gram of tissue, with a lower limit of detection of $10^{1.5}$ $TCID_{50}$/g. The total amount of virus present in each organ was calculated by multiplying the weight of the organ and the viral titer measured in the 10% tissue homogenate.

Statistics. Log-transformed virus titers were compared in a two-tailed *t* test, and statistical significance was assigned to differences with *P* values of <0.05.

Neutralizing-antibody assay. Blood samples were collected from six hamsters on days 0, 7, 14, 21, and 28 following inoculation, and sera were assayed for the presence of SARS CoV-neutralizing antibodies. Twofold dilutions of heat-inactivated sera were tested in a microneutralization assay for the presence of antibodies that neutralized the infectivity of 100 $TCID_{50}$ of SARS CoV in Vero cell monolayers as described previously (23).

Histopathology and IHC. Tissues were placed in 10% neutral buffered formalin and stored at room temperature for at least 3 days. Tissues were subsequently embedded in a paraffin block and processed for routine histology. A colorimetric immunoalkaline phosphatase IHC method was used to identify SARS CoV antigens in tissues as previously described (23). Briefly, rehydrated, deparaffinized tissue sections were digested with proteinase K (Boehringer-Mannheim Corp., Indianapolis, Ind.) and then incubated for 1 h with a hyperimmune mouse ascitic fluid reactive with SARS CoV antigen at a 1:1,000 dilution. After incubation, slides were washed and incubated with a biotinylated anti-mouse antibody. Antigens were visualized by using a streptavidin-alkaline phosphatase complex followed by naphthol-Fast Red substrate for colorimetric detection (DAKO Corp.). Sections were counterstained with Mayer's hematoxylin (Fisher Scientific, Pittsburgh, Pa.).

RESULTS

Replication and clinical response to primary infection with SARS CoV. In a pilot study, efficient viral replication was observed through day 5 p.i. in the respiratory tracts of Golden Syrian hamsters following intranasal administration of 10^3 or 10^5 $TCID_{50}$ of SARS CoV. The viral titers at peak replication in the lungs (day 3 p.i.) were similar regardless of the dose administered (7.5 ± 0.2 $TCID_{50}$/g of lung at both doses). The total amounts of virus recovered on day 1 was $10^{6.5}$ $TCID_{50}$ from lungs and $10^{6.9}$ $TCID_{50}$ from NTs following administration of 10^5 $TCID_{50}$. Similarly, $10^{4.9}$ and $10^{5.2}$ $TCID_{50}$ were recovered on day 1 from lungs and NTs, respectively, following administration of 10^3 $TCID_{50}$. Thus, the total amount of virus present in lungs and NTs at either dose was much greater than the inoculum, indicating that SARS CoV replicates efficiently in the respiratory tract of hamsters.

In a follow-up study, described in detail in this report, Golden Syrian hamsters were inoculated intranasally with 10^3 $TCID_{50}$ of SARS CoV or were mock infected with L15 culture medium. Following inoculation, hamsters were sacrificed at various times and organs were collected for viral titration and histopathology. SARS-inoculated and mock-infected hamsters were weighed every other day and observed for clinical signs of

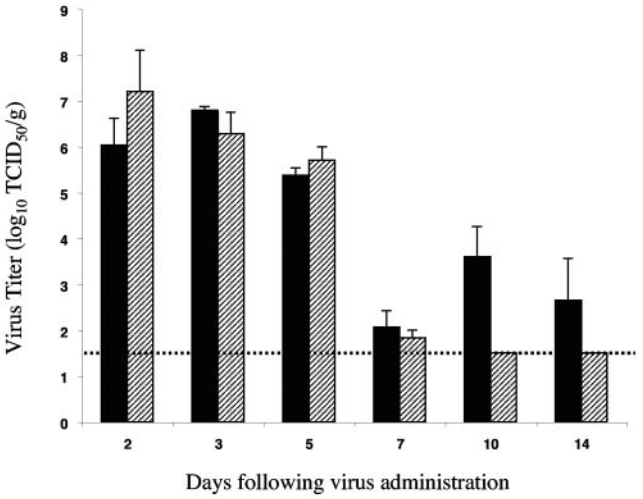

FIG. 1. Replication of SARS CoV in the upper and lower respiratory tracts of hamsters. Virus titers in NTs (solid bars) and lung homogenates (hatched bars) are the mean values calculated from three hamsters per day. Error bars indicate standard errors. The dotted line designates the lower limit of detection ($10^{1.5}$ $TCID_{50}$/g of tissue). Hamsters were inoculated with $10^3$$TCID_{50}$ of SARS CoV on day 0.

TABLE 1. Viral replication in tissues following intranasal administration of 10^3 $TCID_{50}$ of SARS CoV

Organ	Day 2 p.i.			Day 3 p.i.		
	No. positive/ total[a]	Virus titer (mean ± SE)[b]	Total virus present[c]	No. positive/ total	Virus titer (mean ± SE)	Total virus present
Lung	3/3	7.2 ± 0.9	7.1	3/3	6.3 ± 0.5	6.3
NT	3/3	6.0 ± 0.6	5.3	3/3	6.8 ± 0.1	6.1
Liver	2/3	2.5 ± 0.6	2.9	3/3	2.0 ± 0.0	1.7
Spleen	1/3	1.8 ± 0.3	1.9	1/3	1.7 ± 0.2	1.4
Kidney	0/3	≤1.5[d]	ND[e]	0/3	≤1.5[d]	ND

[a] Number of hamsters in which virus was detected in the indicated organ/total number of hamsters evaluated.
[b] Mean viral titers are averages of the values obtained from the three hamsters in each group and are expressed as log_{10} $TCID_{50}$ per gram of tissue.
[c] Total virus present is an average of the titers of virus calculated from whole organs for hamsters in which virus was detected and is expressed as $log_{10}TCID_{50}$/organ.
[d] Lower limit of detection.
[e] ND, none detected.

disease; neither weight loss nor clinical signs of disease were observed. Blood samples were collected weekly from hamsters, and sera were assayed for the presence of SARS CoV-neutralizing antibodies.

Despite the lack of clinical signs of disease, high titers of SARS CoV were detected in the upper and lower respiratory tracts for up to 5 days following virus administration. Virus was not detected in lungs beyond day 7 but was detected at low to moderate levels in NTs of one or more hamsters through day 14 p.i. (Fig. 1).

Histopathology and IHC findings. At 2 days p.i., SARS CoV viral antigens were observed in the respiratory epithelia of the NT (Fig. 2A and B) and trachea (Fig. 2E), including in mucous glands, and occasionally in endothelial cells of the NT (Fig. 2B). Infected epithelial cells of the NT, trachea, and bronchi showed swelling and blebbing of the luminal cytoplasm. Small ulcers were noted in the nasal passages, and focal loss of cilia was noted in the trachea (Fig. 2D). These findings were accompanied by mild mononuclear inflammatory cell infiltrates in the submucosa of the nasal epithelium and bronchioles (Fig. 2A, B, D, and E). In addition, luminal collections of mixed inflammatory cells and necrotic debris associated with viral antigens were seen in nasal passages and bronchioles on day 3. Also, on day 3 p.i., increasing amounts of viral antigens were seen in epithelia of the NT (Fig. 2C) and lungs (Fig. 3B and C) associated with increasing amounts of mononuclear and polymorphonuclear inflammation, seen as multifocal areas of consolidation around bronchioles (Fig. 3A). At day 5 p.i., the damage in the nasal passages had been repaired, NTs showed minimal inflammation, and virus was not detected by IHC staining. Although viral antigens were less abundant in the lungs (Fig. 3E) on day 5 compared to day 3 p.i., progression of the inflammatory reaction in the lungs was observed, with confluence of areas of pneumonic consolidation (Fig. 3D). Consolidation was most extensive at day 7 p.i., affecting up to 30 to 40% of the cut surface in some animals. By day 7 p.i., viral antigens were undetectable in lungs of infected hamsters and inflammation was decreased, while reactive proliferation of epithelial cells was noted (Fig. 4A). By day 14 p.i., lungs were near normal, without detectable viral antigens and with minimal reactive changes, including peribronchial foci of interstitial thickening without inflammation (Fig. 4B).

Extrapulmonary infection. SARS CoV infection disseminated from the respiratory tract early in infection. Transient viremia was detected at low levels 24 h after inoculation and reached a titer of 10^3 $TCID_{50}$/ml of plasma by day 2 p.i., but it was not detected on day 3 p.i. Detection of SARS CoV in endothelial cells by IHC (Fig. 2B) fits with the observation of viremia. At 2 and 3 days p.i., low titers of virus were detected in homogenates of the liver and spleen. Virus was not detected in liver or spleen after day 3 and was not recovered from the kidneys at any point during the study (Table 1). Despite multiple attempts, it was difficult to isolate SARS CoV from the intestines because high levels of bacterial contamination and protease activity were cytopathic for the Vero cell monolayers. Histopathological evaluation of the spleen, liver, kidney, and gastrointestinal tract showed no evidence of inflammation or presence of SARS CoV antigens (data not shown).

SARS CoV-specific humoral immune response. Neutralizing antibodies specific for SARS CoV were detected in SARS-inoculated hamsters as early as day 7 p.i. (Fig. 5). The titers of serum neutralizing antibodies to SARS CoV at the time of challenge were very high (mean, 1:436) and provided complete protection from virus replication in the lower respiratory tract and an impressive 100,000-fold reduction of virus titers in the NTs (Table 2).

Protection from SARS CoV challenge. Hamsters that had recovered from primary infection were protected from challenge with SARS CoV at day 28, as indicated by greatly decreased virus replication (Table 2), a lack of detectable viral antigen, and the absence of pneumonitis (Fig. 4C). Virus was detected at very low titer in the upper respiratory tract of a single hamster (Table 2), which may represent residual viral inoculum. The hamsters showed no evidence of infection in the liver or spleen. In contrast, high titers of virus were detected in

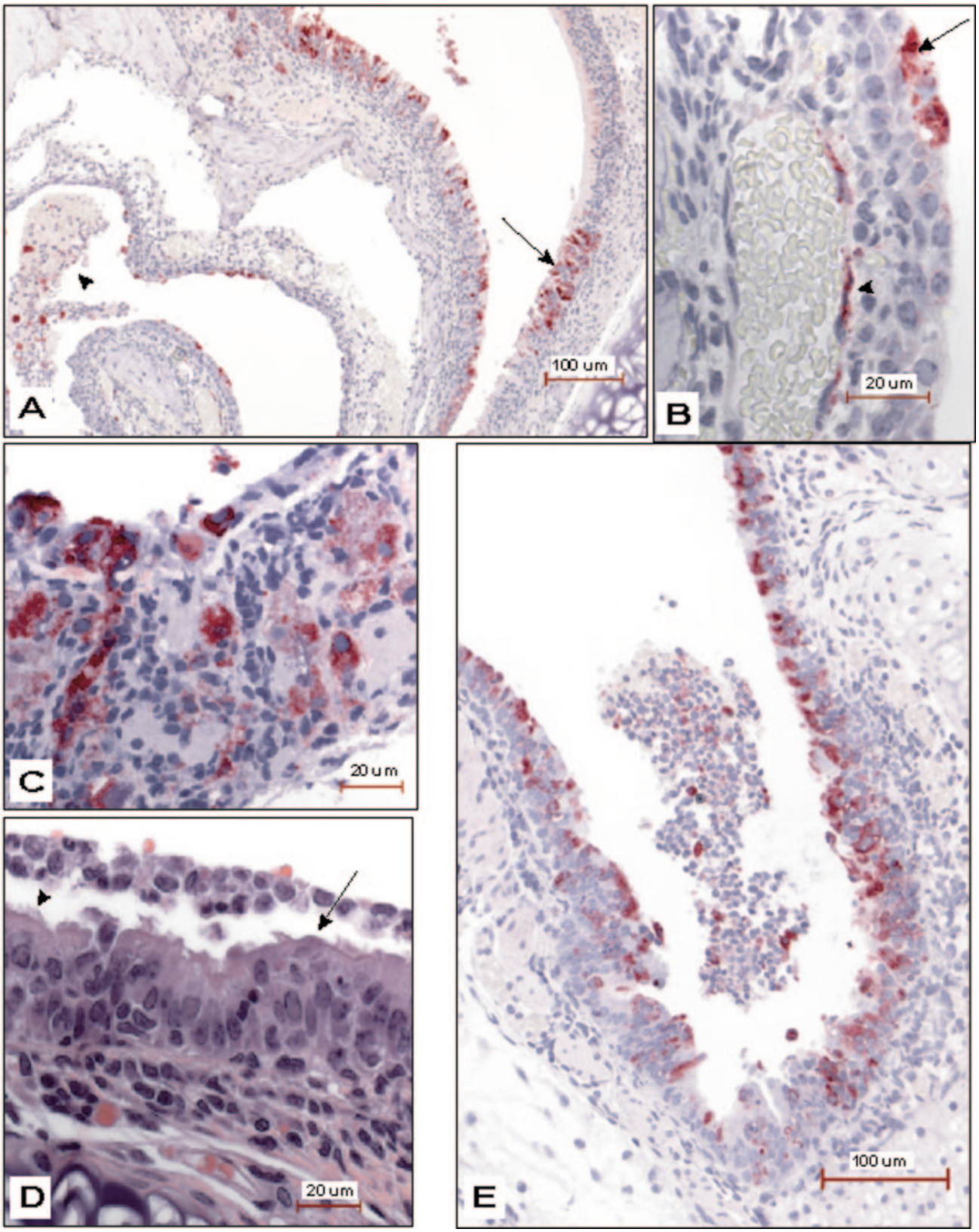

FIG. 2. Pathology in NTs and tracheae of hamsters at days 2 and 3 of SARS CoV infection. NTs at day 2 p.i. show the presence of SARS CoV antigens (red) in cells of the epithelial surface lining (arrows in A and B), necrotic debris in the nasal passages (arrowhead in A), and endothelial cells (arrowhead in B). The mononuclear nature of the inflammatory cell infiltrate is seen in B. NTs at day 3 p.i. show mononuclear inflammatory infiltrate in the submucosa and the presence of SARS CoV antigens (red) in cells of the epithelial surface lining and in mucous glands (C). The trachea at day 2 p.i. shows tracheal epithelial cells with loss of the apical portion of the cytoplasm including cilia (arrow in D; compare to arrowhead, where cilia are still present), debris with desquamated epithelial and inflammatory cells in the lumen, and submucosal mononuclear inflammatory infiltrate (D and E). SARS CoV antigens (red) are observed in the epithelial cells of the trachea (E) at 2 days p.i. and are accompanied by mild inflammatory infiltrate. A, B, C, and E, IHC assays; D, hematoxylin-and-eosin stain.

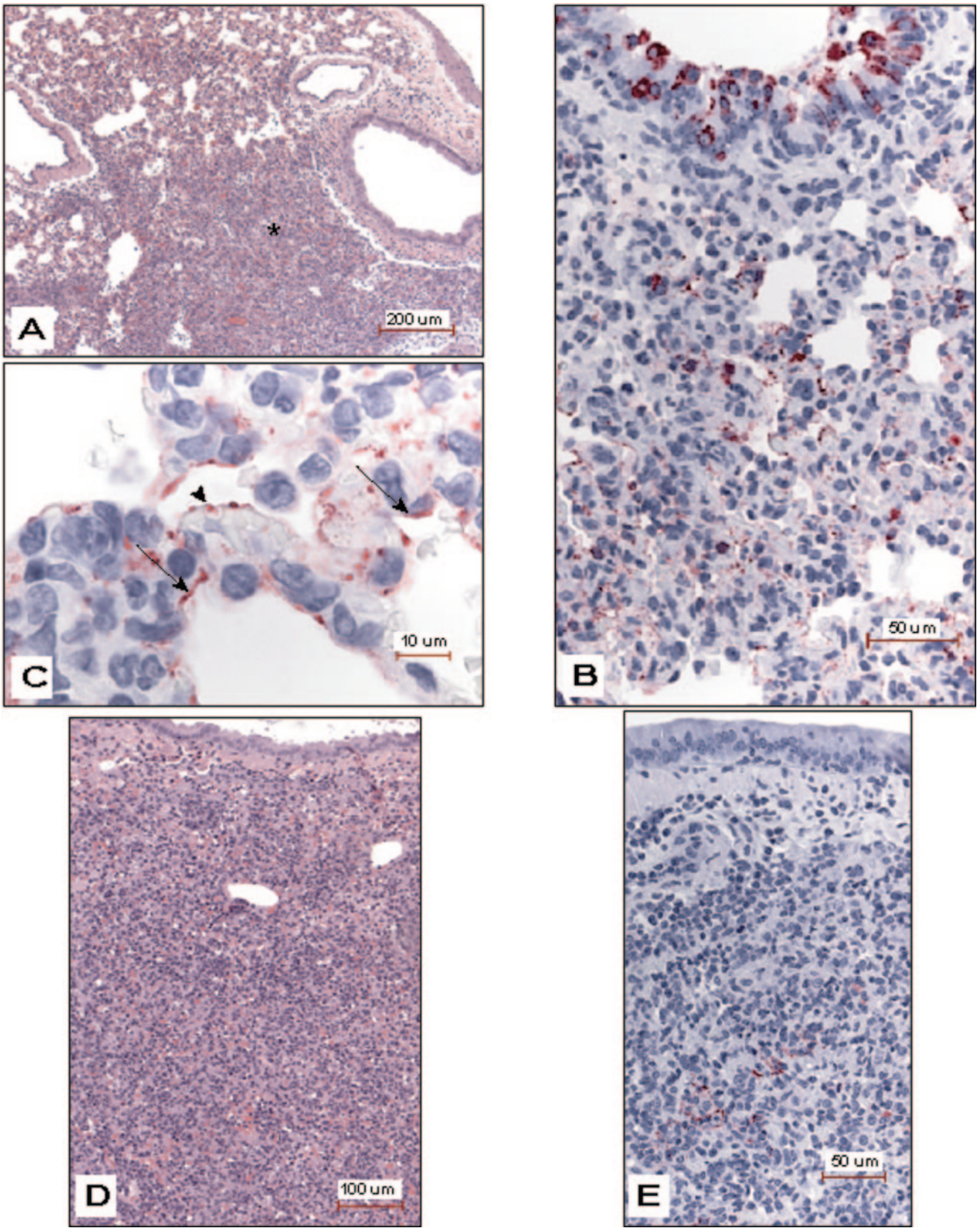

FIG. 3. Pathology in hamster lungs at days 3 and 5 of SARS CoV infection. The lung at 3 days p.i. shows focal pneumonic consolidation around bronchi (asterisk in A). SARS CoV antigens (red) are noted in bronchial epithelium and in consolidated areas of the lung (B), which at higher magnification are seen inside alveolar lining cells (pneumocytes; arrow in C) and possibly in endothelial cells (arrowhead in C). The inflammatory infiltrate at 3 days p.i. is localized to the alveolar septal walls (B and C). The lung at 5 days p.i. shows confluent pneumonic consolidation (D) and decreasing amounts of SARS CoV antigens (red) in both consolidated areas and bronchial epithelium (E). A and D, hematoxylin-and-eosin stain; B, C, and E, IHC assays.

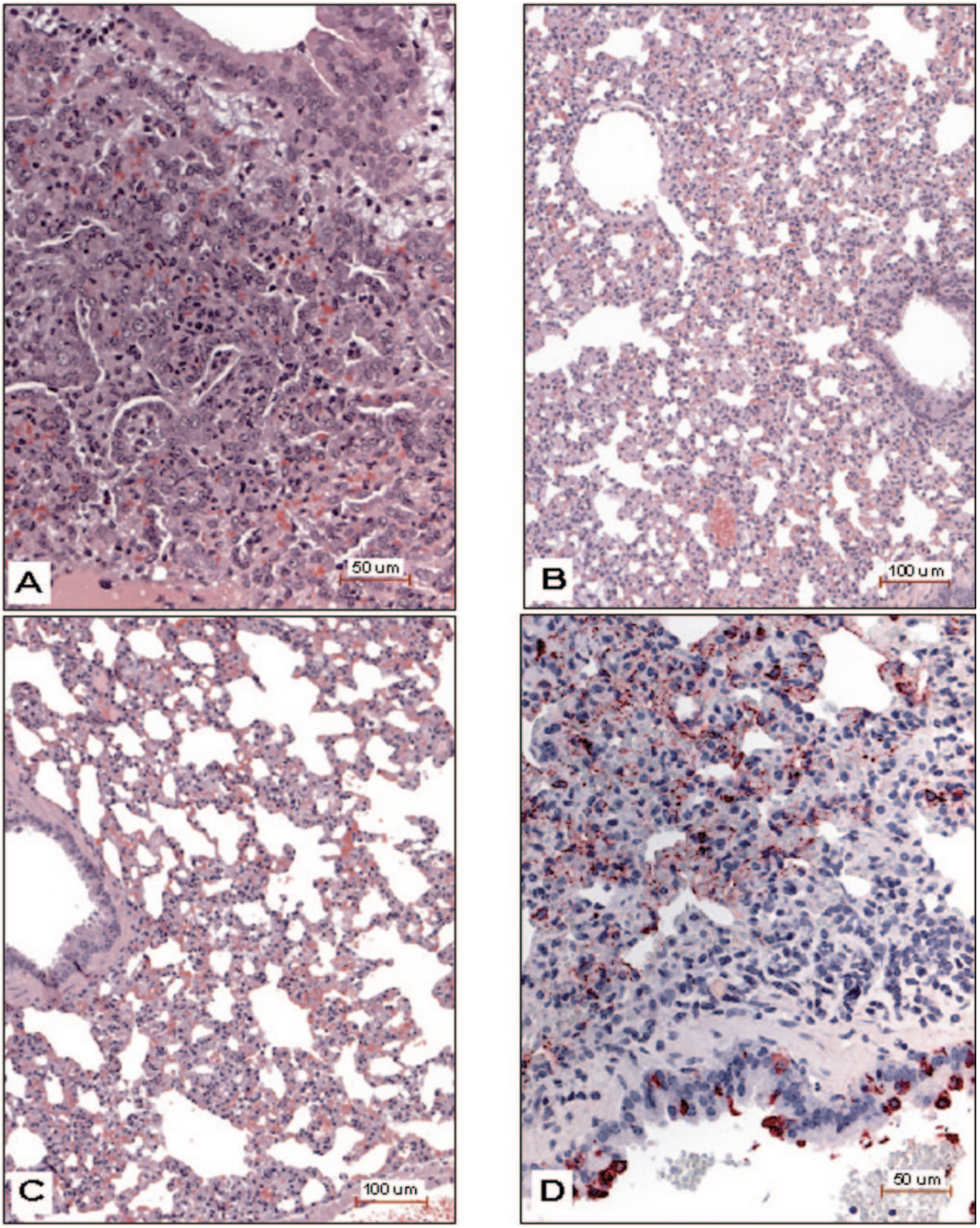

FIG. 4. Pathology in hamster lungs at days 7 and 14 of SARS CoV infection and after challenge. The lung at 7 days p.i. shows a decrease of the inflammatory infiltrate in the alveolar septae and proliferation of reparative cuboidal epithelial cells lining slender air spaces (A). The lung at 14 days p.i. shows normal alveolar air spaces with minimal amounts of thickening of the alveolar septae (B). The lung 3 days after SARS CoV rechallenge shows normal alveolar air spaces and no pneumonic consolidation (C). In contrast, SARS CoV antigens (red) are observed in the bronchial epithelium and in the peribronchial pneumonic consolidations (D) of the lung of a hamster that was mock infected initially and sacrificed 3 days after challenge with SARS CoV, similar to what was seen at day 3 p.i. (Fig. 3A, B, and C). A, B, and C, hematoxylin-and-eosin stain; D, IHC assay.

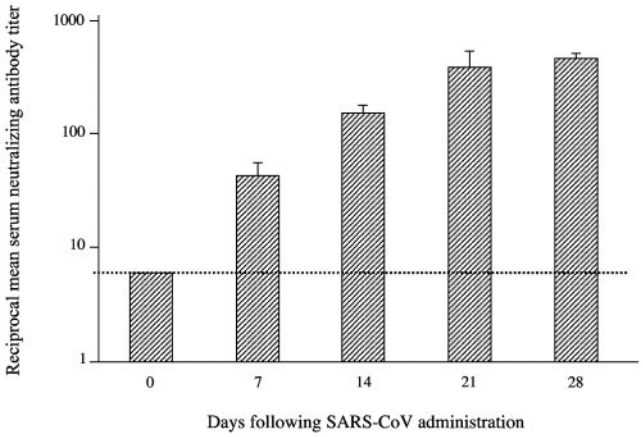

FIG. 5. Reciprocal SARS CoV-specific serum neutralizing-antibody titers in SARS-infected hamsters on the indicated days following intranasal inoculation. Mean antibody titers from three hamsters per group are shown on a logarithmic scale. Error bars indicate standard errors. The dotted line indicates the lower limit of detection (<1:8).

the upper and lower respiratory tracts of a control group of hamsters that had been mock infected on day 0 and were challenged with SARS CoV on day 28 (Table 2). Histopathological and IHC findings for these hamsters (Fig. 4D) were similar to those seen on day 3 following primary infection as described above (Fig. 3A and B). An additional five Golden Syrian hamsters were observed for 33 days following a homologous SARS CoV challenge administered 8 weeks after an initial inoculation with SARS CoV. Clinical signs of illness were not observed in SARS-rechallenged hamsters.

DISCUSSION

Animal models, critical for preclinical evaluation of the safety, immunogenicity, and efficacy of candidate vaccines, that have been described for SARS include nonhuman primates, ferrets, and mice (14, 16, 23). While many candidate vaccines are being developed, an ideal animal model in which clinical disease and pathological findings consistent with human disease are present is still lacking. In the absence of clinical disease, animal models such as hamsters that develop histopathological evidence of pneumonia in association with virus replication can be useful for evaluation of vaccines and antiviral therapy. The hamster provides several benefits over previously reported models.

The report indicating that SARS CoV fulfilled Koch's postulates described lethargy, skin rash, and respiratory distress in cynomolgus macaques following introduction on the conjunctiva and intranasal and intratracheal administration of SARS CoV (14). That study reported viral replication in tissues (detected by reverse transcription-PCR) and interstitial pneumonia 6 days following virus administration. We examined the level of SARS CoV replication in the upper and lower respiratory tracts of rhesus and cynomolgus macaques and African green monkeys (AGMs) and found that the virus replicates to a higher titer and for a longer duration in AGMs than in the macaques, indicating that they are a better model than macaques (16a). However, none of these monkeys demonstrated

TABLE 2. Prior infection prevents replication of SARS CoV following challenge

Primary infection	Serum neutralizing-antibody titer[a]	Mean virus titer ($\log_{10}$ $TCID_{50}$/g) ± SE in[b]:			
		NT	Lung	Liver	Spleen
SARS CoV	1:436	1.8 ± 0.3	≤1.5 ± 0.0[c]	≤1.5 ± 0.0[c]	≤1.5 ± 0.0[c]
Mock	≤1:8[c]	7.5 ± 0.0*	8.0 ± 0.2**	3.1 ± 0.8†	2.2 ± 0.7†

[a] Mean serum neutralizing-antibody titer present on day 28 prior to administration of challenge dose of SARS CoV.
[b] SARS CoV (10^3 $TCID_{50}$) was administered intranasally 28 days following primary infection; tissues were harvested 3 days later. Titers represent averages obtained from three hamsters/group. *, $P = 0.004$; **, $P = 0.0007$; †, $P > 0.05$.
[c] Lower limit of detection.

any clinical signs of disease, and the duration of viral replication was short even in AGMs. We believe that the use of these nonhuman primate species as models for SARS must be carefully considered because of the variability of the level of viral replication between animals and the short duration of replication even in productive infections. This is in strong contrast to the high-titer virus replication and extended duration of replication consistently observed in hamsters.

Ferrets are valuable models for the study of influenza viruses because they develop a clinical illness that resembles human influenza, with rhinorrhea, fever, and sneezing following intranasal infection (11), and therefore they were investigated as a possible model for SARS (16). Virus replication and pneumonitis were observed in ferrets that were infected intranasally with SARS CoV. The experimentally infected ferrets did not develop fever or respiratory signs but were lethargic. The histopathological findings in the lungs of ferrets were described as similar to but milder than those seen in cynomolgus macaques (16). Both hamsters and ferrets support virus replication in the respiratory tract and develop pathological evidence of disease, but hamsters appear to support more efficient replication of SARS CoV than ferrets and have very pronounced pathological findings in acute infection and during viral clearance and tissue repair. Although the methodology used in the paper describing the ferret model differs from that used in our study, the mean peak titer of SARS CoV observed in the upper respiratory tracts of hamsters is $10^{6.8}$ $TCID_{50}$/g of tissue at 3 days after intranasal administration of 10^3 $TCID_{50}$ of SARS CoV. In contrast, the mean peak titer in pharyngeal swabs of ferrets was $\sim 10^5$ $TCID_{50}$/ml at 4 days after intratracheal administration of 10^6 $TCID_{50}$ of SARS CoV. The histopathological findings in the ferret and hamster models cannot be directly compared because details of the lung pathology seen in ferrets are not available. Hamsters are small, outbred animals that are more readily available than either nonhuman primates or ferrets, and they develop histopathological changes along with consistently high levels of viral replication following SARS CoV infection.

We have recently reported efficient replication of SARS CoV in the respiratory tracts of inbred, 4- to 6-week old BALB/c mice, in the absence of associated pathology or clinical disease (23). The kinetics of SARS CoV replication in hamsters are similar to those seen in mice and resemble the pattern of viral replication observed in hamsters following inoculation with other respiratory viruses, e.g., influenza A and parainfluenza viruses (11, 22). We have demonstrated replica-

tion of the virus in epithelial cells of the respiratory tracts of mice and hamsters. The virus replicates more efficiently in hamsters than in mice, and, possibly as a result of greater antigenic stimulation, the neutralizing-antibody response in hamsters is more robust than that in mice (23). In contrast to the BALB/c mouse model, in which virus is detected only in the respiratory tract and is cleared by day 5, hamsters demonstrate a longer duration of viral shedding from the upper respiratory tract, a transient viremia, spread to extrapulmonary tissues, and most significantly, inflammation in the respiratory tract associated with viral replication. Furthermore, the presence of pneumonitis observed in hamsters following primary SARS CoV infection provides a model that permits an evaluation of aspects of potential disease enhancement following SARS CoV reinfection.

Feline infectious peritonitis virus (FIPV) is a group I coronavirus that causes severe morbidity and mortality in cats, and it has been shown that preexisting antibody to FIPV may enhance subsequent FIPV infection and accelerate both morbidity and mortality (25). In FIPV, Fc receptor-mediated infection of macrophages is believed to be an important mechanism underlying disease enhancement. Although this antibody-dependent enhancement appears to be limited to FIPV among coronaviruses, the development of enhanced disease in the presence of preexisting antibody to SARS CoV would be of concern. Disease enhancement was not observed in our studies; i.e., signs of clinical illness, increased viral replication, or histopathological findings were not observed after rechallenge. In hamsters, SARS CoV was found predominantly in epithelial cells, pneumocytes, and occasionally in vascular endothelial cells. The lack of detectable viral replication and pathology 3 days after SARS CoV challenge in hamsters with neutralizing-antibody titers of >1:400 suggests that it is highly unlikely that antibody-mediated disease enhancement will be observed for SARS CoV. More extensive studies that will seek indications of clinical illness such as weight loss and examine viral replication and histopathological findings beyond day 3 postchallenge are planned.

Most tissues studied from SARS-infected humans are derived from autopsies of patients who had been ill for more than 2 weeks, and very few are from earlier time points. Human SARS CoV-infected lungs show diffuse alveolar damage characterized by desquamation of epithelial cells, fibrin and collagen deposits in the alveolar space, hyperplasia of type II pneumocytes, increased mononuclear infiltrates in the interstitium, and in some cases the presence of multinucleated syncytial cells (9, 13). Detection of viral nucleic acids and antigens in human tissues varies with the duration of illness (3, 20). SARS CoV antigen and nucleic acid were not detected in patients with prolonged illness; however, in the small number of patients studied who had a short (1-week) duration of illness, virus was detected in pneumocytes, occasionally in macrophages, in intraalveolar necrotic debris within the alveolar septal walls, and rarely in bronchoepithelial cells. The late-stage histopathology in hamsters is analogous to that described for humans late in the course of illness. In this context, the early histopathological and IHC changes observed in the hamsters may shed light upon the early events in SARS infection. Examination of hamster tissues demonstrated a sequence of events that begins with the presence of SARS CoV antigens primarily in the respiratory epithelium associated with minimal inflammatory reaction. The presence of SARS CoV in the nasal epithelia of hamsters correlates with what is seen with other coronaviruses (1). This is followed by the presence of viral antigen in alveolar epithelium accompanied by focal and later generalized pneumonic consolidation as amounts of antigen in the trachea and bronchi decrease, and the process ends with viral clearance and repair of damaged tissues.

In summary, although clinical symptoms consistent with SARS in humans are absent, as they are in murine, ferret, and most simian models, Golden Syrian hamsters provide an excellent small animal model for acute SARS CoV replication and associated pathology and provide insights into the early events in SARS CoV infection. The hamster model demonstrates high titers of virus accompanied by associated pathology in the upper and lower respiratory tracts and evidence of virus in extrapulmonary sites following intranasal infection. The humoral immune response, as measured by mean serum neutralizing-antibody titers 28 days after virus administration, is also more robust in hamsters (1:436) than in African green monkeys (1:57) or mice (1:49). Hamsters infected with SARS CoV are protected from subsequent infection and show no clinical signs of disease following homologous challenge. The efficacy of candidate vaccines, immunotherapy, or antiviral agents can be evaluated in the hamster model by measuring the ability of these interventions to prevent virus replication and associated pathology following challenge. The availability of a rodent model in which virus replication is accompanied by pneumonia should expand and expedite research in the evaluation of SARS immunoprophylaxis and therapy.

ACKNOWLEDGMENTS

Special thanks go to Josephine McAuliffe and Nadia Naffakh for their support and technical assistance and to personnel at Bioqual, Inc., Rockville, Md., for their care and handling of hamsters used in this study. Special thanks also go to Christopher Paddock and Wun-Ju Shieh (Infectious Disease Pathology Activity, Centers for Disease Control and Prevention) for consultation on histopathological findings, to Pierre Rollin for the anti-SARS CoV antibody, and to Mitesh Patel for aiding in the layout of hematoxylin-eosin and IHC figures.

REFERENCES

1. **Afzelius, B. A.** 1994. Ultrastructure of human nasal epithelium during an episode of coronavirus infection. Virchows Archiv. **424:**295–300.
2. **Bukreyev, A., E. W. Lamirande, U. J. Buchholz, L. N. Vogel, W. R. Elkins, M. St. Claire, B. R. Murphy, K. Subbarao, and P. L. Collins.** 2004. Mucosal immunisation of African green monkeys (Cercopithecus aethiops) with an attenuated parainfluenza virus expressing the SARS coronavirus spike protein for the prevention of SARS. Lancet **363:**2122–2127.
3. **Chong, P. Y., P. Chui, A. E. Ling, T. J. Franks, D. Y. Tai, Y. S. Leo, G. J. Kaw, G. Wansaicheong, K. P. Chan, L. L. Ean Oon, E. S. Teo, K. B. Tan, N. Nakajima, T. Sata, and W. D. Travis.** 2004. Analysis of deaths during the severe acute respiratory syndrome (SARS) epidemic in Singapore: challenges in determining a SARS diagnosis. Arch. Pathol. Lab. Med. **128:**195–204.
4. **Donoghue, M., F. Hsieh, E. Baronas, K. Godbout, M. Gosselin, N. Stagliano, M. Donovan, B. Woolf, K. Robison, R. Jeyaseelan, R. E. Breitbart, and S. Acton.** 2000. A novel angiotensin-converting enzyme-related carboxypeptidase (ACE2) converts angiotensin I to angiotensin 1–9. Circulation Res. **87:**1–9.
5. **Drosten, C., S. Gunther, W. Preiser, S. van der Werf, H. R. Brodt, S. Becker, H. Rabenau, M. Panning, L. Kolesnikova, R. A. Fouchier, A. Berger, A. M. Burguiere, J. Cinatl, M. Eickmann, N. Escriou, K. Grywna, S. Kramme, J. C. Manuguerra, S. Muller, V. Rickerts, M. Sturmer, S. Vieth, H. D. Klenk, A. D. Osterhaus, H. Schmitz, and H. W. Doerr.** 2003. Identification of a novel coronavirus in patients with severe acute respiratory syndrome. N. Engl. J. Med. **348:**1967–1976.
6. **Durbin, A. P., M. H. Skiadopoulos, J. M. McAuliffe, J. M. Riggs, S. R.**

Surman, P. L. Collins, and B. R. Murphy. 2000. Human parainfluenza virus type 3 (PIV3) expressing the hemagglutinin protein of measles virus provides a potential method for immunization against measles virus and PIV3 in early infancy. J. Virol. **74:**6821–6831.

7. **Federal Register.** 2002. New drug and biological drug products; evidence needed to demonstrate effectiveness of new drugs when human efficacy studies are not ethical or feasible. Fed. Regist. **67:**37988–37998.
8. **Fouchier, R. A., T. Kuiken, M. Schutten, G. van Amerongen, G. J. van Doornum, B. G. van den Hoogen, M. Peiris, W. Lim, K. Stohr, and A. D. Osterhaus.** 2003. Aetiology: Koch's postulates fulfilled for SARS virus. Nature **423:**240.
9. **Franks, T. J., P. Y. Chong, P. Chui, J. R. Galvin, R. M. Lourens, A. H. Reid, E. Selbs, C. P. McEvoy, C. D. Hayden, J. Fukuoka, J. K. Taubenberger, and W. D. Travis.** 2003. Lung pathology of severe acute respiratory syndrome (SARS): a study of 8 autopsy cases from Singapore. Hum. Pathol. **34:**743–748.
10. **Guan, Y., B. J. Zheng, Y. Q. He, X. L. Liu, Z. X. Zhuang, C. L. Cheung, S. W. Luo, P. H. Li, L. J. Zhang, Y. J. Guan, K. M. Butt, K. L. Wong, K. W. Chan, W. Lim, K. F. Shortridge, K. Y. Yuen, J. S. M. Peiris, and L. L. M. Poon.** 2003. Isolation and characterization of viruses related to the SARS coronavirus from animals in Southern China. Science **302:**276–278.
11. **Herlocher, M. L., S. Elias, R. Truscon, S. Harrison, D. Mindell, C. Simon, and A. S. Monto.** 2001. Ferrets as a transmission model for influenza: sequence changes in HA1 of type A (H3N2) virus. J. Infect. Dis. **184:**542–546.
12. **Komatsu, T., Y. Suzuki, J. Imai, S. Sugano, M. Hida, A. Tanigami, S. Muroi, Y. Yamada, and K. Hanaoka.** 2002. Molecular cloning, mRNA expression and chromosomal localization of mouse angiotensin-converting enzyme-related carboxypeptidase (mACE2). DNA Sequence **13:**217–220.
13. **Ksiazek, T. G., D. Erdman, C. S. Goldsmith, S. R. Zaki, T. Peret, S. Emery, S. Tong, C. Urbani, J. A. Comer, W. Lim, P. E. Rollin, S. F. Dowell, A. E. Ling, C. D. Humphrey, W. J. Shieh, J. Guarner, C. D. Paddock, P. Rota, B. Fields, J. DeRisi, J. Y. Yang, N. Cox, J. M. Hughes, J. W. LeDuc, W. J. Bellini, L. J. Anderson, et al.** 2003. A novel coronavirus associated with severe acute respiratory syndrome. N. Engl. J. Med. **348:**1953–1966.
14. **Kuiken, T., R. A. M. Fouchier, M. Schutten, G. F. Rimmelzwaan, G. van Amerongen, D. van Riel, J. D. Laman, T. de Jong, G. van Doornum, W. Lim, A. E. Ling, P. K. S. Chan, J. S. Tam, M. C. Zambon, R. Gopal, C. Drosten, S. van der Werf, N. Escriou, J. C. Manuguerra, K. Stohr, J. S. M. Peiris, and A. D. M. E. Osterhaus.** 2003. Newly discovered coronavirus as the primary cause of severe acute respiratory syndrome. Lancet **362:**263–270.
15. **Li, W., M. J. Moore, N. Vasilieva, J. Sui, S. K. Wong, M. A. Berne, M. Somasundaran, J. L. Sullivan, K. Luzuriaga, T. C. Greenough, H. Choe, and M. Farzan.** 2003. Angiotensin-converting enzyme 2 is a functional receptor for the SARS coronavirus. Nature **426:**450–454.
16. **Martina, B. E. E., B. L. Haagmans, T. Kuiken, R. A. M. Fouchier, G. F. Rimmelzwaan, G. V. Amerongen, J. S. M. Peiris, W. Lim, and A. D. M. E. Osterhaus.** 2003. SARS virus infection of cats and ferrets. Nature **425:**915.

16a. **McAuliffe, J., L. Vogel, A. Roberts, G. Fahle, S. Fisher, W.-J. Shieh, E. Butler, S. Zaki, M. St. Claire, B. Murphy, and K. Subbarao.** 2004. Replication of SARS coronavirus administered into the respiratory tract of African green, rhesus and cynomolgus monkeys. Virology **330:**8–15.

17. **Ng, S. K. C.** 2003. Possible role of an animal vector in the SARS outbreak at Amoy Gardens. Lancet **362:**570–572.
18. **Peiris, J. S., S. T. Lai, L. L. Poon, Y. Guan, L. Y. Yam, W. Lim, J. Nicholls, W. K. Yee, W. W. Yan, M. T. Cheung, V. C. Cheng, K. H. Chan, D. N. Tsang, R. W. Yung, T. K. Ng, K. Y. Yuen, et al.** 2003. Coronavirus as a possible cause of severe acute respiratory syndrome. Lancet **361:**1319–1325.
19. **Schmidt, A. C., D. R. Wenzke, J. M. McAuliffe, M. St Claire, W. R. Elkins, B. R. Murphy, and P. L. Collins.** 2002. Mucosal immunization of rhesus monkeys against respiratory syncytial virus subgroups A and B and human parainfluenza virus type 3 by using a live cDNA-derived vaccine based on a host range-attenuated bovine parainfluenza virus type 3 vector backbone. J. Virol. **76:**1089–1099.
20. **Shieh, W.-J., C. H. Hsiao, C. Paddock, J. Guarner, L. Mueller, C. S. Goldsmith, K. Tatti, M. Packard, I. J. Su, and S. R. Zaki.** Immunohistochemical, in situ hybridization, and ultrastructural localization of SARS-associated coronavirus in a fatal case of severe acute respiratory syndrome in Taiwan. Submitted for publication.
21. **Skiadopoulos, M. H., S. Biacchesi, U. J. Buchholz, J. M. Riggs, S. R. Surman, E. Amaro-Carambot, J. M. McAuliffe, W. R. Elkins, M. St. Claire, P. L. Collins, and B. R. Murphy.** 2004. The two major human metapneumovirus genetic lineages are highly related antigenically, and the fusion (F) protein is a major contributor to this antigenic relatedness. J. Virol. **78:**6927–6937.
22. **Subbarao, E. K., E. J. Park, C. M. Lawson, A. Y. Chen, and B. R. Murphy.** 1995. Sequential addition of temperature-sensitive missense mutations into the PB2 gene of influenza A transfectant viruses can effect an increase in temperature sensitivity and attenuation and permits the rational design of a genetically engineered live influenza A virus vaccine. J. Virol. **69:**5969–5977.
23. **Subbarao, K., J. McAuliffe, L. Vogel, G. Fahle, S. Fischer, K. Tatti, M. Packard, W.-J. Shieh, S. Zaki, and B. Murphy.** 2004. Prior infection and passive transfer of neutralizing antibody prevent replication of SARS coronavirus in the respiratory tract of mice. J. Virol. **78:**3572–3577.
24. **Tao, S. C., D. Jiang, H. L. Lu, W. L. Xing, Y. X. Zhou, and J. Cheng.** 2004. One-tube nested RT-PCR enabled by using a plastic film and its application for the rapid detection of SARS-virus. Biotechnol. Lett. **26:**179–183.
25. **Weiss, R. C., W. J. Dodds, and F. W. Scott.** 1980. Disseminated intravascular coagulation in experimentally induced feline infectious peritonitis. Am. J. Vet Res. **41:**663–671.
26. **Zhong, N. S., B. J. Zheng, Y. M. Li, X. Z. H. Poon, K. H. Chan, P. H. Li, S. Y. Tan, Q. Chang, J. P. Xie, X. Q. Liu, J. Xu, D. X. Li, K. Y. Yuen, and G. Y. Peiris.** 2003. Epidemiology and cause of severe acute respiratory syndrome (SARS) in Guangdong, People's Republic of China, in February, 2003. Lancet **362:**1353–1358.